Phen-Gen: combining phenotype and genotype to analyze rare disorders

Asif Javed, Saloni Agrawal & Pauline C Ng

We introduce Phen-Gen, a method that combines patients' disease symptoms and sequencing data with prior domain knowledge to identify the causative genes for rare disorders. Simulations revealed that the causal variant was ranked first in 88% of cases when it was a coding variant—a 52% advantage over a genotype-only approach—and Phen-Gen outperformed other existing prediction methods by 13–58%. If disease etiology was unknown, the causal variant was assigned the top rank in 71% of simulations. Phen-Gen is available at http://phen-gen.org/.

Diagnosis of rare disorders based on high-throughput sequencing in large clinical studies remains moderate, varying between 16% and 50% (refs. 1,2). In two-thirds of new cases, the cause remains unknown[3], and nearly half of the disorders reported in the compendium Online Mendelian Inheritance in Man (OMIM) have an unknown molecular basis[4]. Issues that may be limiting the success of a study include a focus on coding exome with exclusion of potential regulatory variants[5] and a lack of systematic integration of prior knowledge of the disease and genes involved.

Phen-Gen is a method that combines a patient's sequencing data and symptoms with prior knowledge of human diseases and functional interplay of different genes, all within a systematic Bayesian framework (**Supplementary Fig. 1**). The patient symptoms are semantically matched against a database of known human disorders using an in-house implementation of Phenomizer[6]. The potential role of novel (previously uncharacterized) but functionally similar genes is estimated using a random walk–with–restart algorithm over a gene interaction network. This network was constructed by integrating seven data sources (Online Methods). We analyzed the sequencing data using an exome-centric approach and a genomic approach. Phen-Gen's exome-centric approach predicts the damaging impact of coding mutations using nonsynonymous, splice-site and indel predictors within a unifying framework (**Supplementary Figs. 2** and **3**). This allows for a direct quantitative comparison between coding variants.

Phen-Gen's genome-wide approach utilizes evolutionary conservation, Encyclopedia of DNA Elements (ENCODE)-predicted functionality and proximity to coding sequence to estimate a locus's susceptibility for disease (**Supplementary Figs. 4** and **5**). Both the exome-centric and genomic approaches take into account that healthy humans harbor hundreds of supposedly damaging mutations and that certain genes are more prone to these so-called deleterious variants (**Supplementary Fig. 6**).

The performances of Phen-Gen's predictors for exome and genome have been quantified using enrichment of disease-causal mutations in conjunction with depletion of common polymorphisms. We combined the phenotypic and genotypic predictions and ranked genes on the basis of the two corroboratory pieces of evidence.

As a safeguard against overfitting, each component of our loosely coupled pipeline was individually evaluated in cross-validation before we analyzed the complete method in totality. Phen-Gen assigned the causal gene first rank in 88% of simulations. It showed a 19–58% improvement in direct simulation comparison to the previously published methods eXtasy[7], VAAST[8] and PHEVOR[9] and 13–16% improvement over results reported by PHIVE[10] in a comparable simulation framework. For novel genes unknown to our internal database, Phen-Gen assigned first rank in 71% of simulations. The efficacy of Phen-Gen is further established in real patient data from a recently published study[1]: the causal gene was ranked first in 8 of 11 patients (and within the top five in all patients). For ease of use and to address data privacy issues, Phen-Gen is available as both a web server and an open-source downloadable package (http://phen-gen.org/).

When evaluating the method at the level of disease variants across different subclasses reported in the Human Gene Mutation Database[11] (HGMD 2011.4) (**Supplementary Fig. 7**), we saw that in all three coding categories, at least 84% of mutations were predicted to be damaging with high probability (≥0.9). The genomic predictor was evaluated using HGMD-reported disease-causal regulatory variants; 80% were scored, and 38% were assigned a damaging probability of 0.5 or higher.

We then evaluated Phen-Gen with *in silico* patients. For a given disorder, a patient's genetic data were created by adding an HGMD disease-causal mutation into a healthy individual's genome or exome. The patient's phenotypic data were generated on the basis of reported disease symptoms. Combining all dominant and recessive simulations, Phen-Gen assigned the disease-causal variant first rank in 88% of the cases across different classes of coding variants (**Table 1** and **Supplementary Table 1**).

To ascertain the performance in implicating novel causal genes, we split the HGMD-reported variants by whether the disease-gene link was 'known' or 'unknown' to our local Phenomizer database. When the gene was known, Phen-Gen assigned it the first rank in 92% of cases for dominant and 96% of cases for recessive diseases (**Table 1**). However, even for unknown disorders, adding

Computational and Systems Biology Group, Genome Institute of Singapore, Agency for Science, Technology and Research, Singapore. Correspondence should be addressed to A.J. (javeda@gis.a-star.edu.sg) or P.C.N. (ngpc4@gis.a-star.edu.sg).

RECEIVED 1 APRIL; ACCEPTED 16 JUNE; PUBLISHED ONLINE 3 AUGUST 2014; DOI:10.1038/NMETH.3046

Table 1 | Performance in simulated patients for coding predictor

	Dominant			Recessive		
	Top gene (%)	Top 5 genes (%)	Top 10 genes (%)	Top gene (%)	Top 5 genes (%)	Top 10 genes (%)
Combined (missense, nonsense, splice site and indels)						
Phen-Gen	81	88	91	96	97	97
Genotype only	0	3	13	72	97	97
Phenotype only	31	69	74	24	51	68
Known	92	97	97	96	97	97
Unknown	43	61	73	92	96	96

Phen-Gen's performance is evaluated with Online Mendelian Inheritance in Man (OMIM)-listed disease symptoms and Human Gene Mutation Database (HGMD)-reported variants for coding predictor. Across all simulations, Phen-Gen assigns the causal variant top rank in 88% of cases. The table entries reflect the percentage of simulations in each category with the indicated result. The top three rows represent the performance of the complete method (genotype and phenotype), the genotype-only approach and the phenotype-only approach, respectively. The performance of Phen-Gen when the causal gene is previously known and unknown is depicted as well.

the disease symptoms enabled Phen-Gen to correctly identify the true gene in 43% of dominant and 92% of recessive disorders. To further evaluate Phen-Gen's role in novel disease-gene discovery, we masked the gene's association with the disorder in the respective simulation. The results were comparable to those with the true unknown cases. Combining results from all unknown and masked simulations, Phen-Gen was able to assign first rank to disease-causal variants in 71% cases (**Supplementary Table 2**).

To evaluate any potential biases of using 1000 Genomes data for both allele frequency estimation and generating *in silico* patients, we repeated the simulations using only Exome Sequencing Project[12] data in the common-variant filtration step (**Supplementary Table 3**). We also evaluated the performance of our method in identifying the disease-causal gene with a compound heterozygous disease-inheritance pattern (**Supplementary Table 4** and **Supplementary Fig. 8**). Moreover, to account for phenotypic heterogeneity, Phen-Gen was assessed by randomly sampled symptoms from 44 disorders for which the symptom list and their frequency of occurrence has been compiled[6] (**Supplementary Table 5** and **Supplementary Fig. 9**).

It is more challenging to narrow down the role of a particular noncoding variant in a rare disorder. Phen-Gen correctly identified the genetic cause in 49% of cases with noncoding disease variants, with phenotypic information contributing substantially to the prediction (**Supplementary Table 6**). Moreover, the decoupled nature of the phenotypic and genotypic predictors within the unifying analysis framework bodes well for improving predictions as the regulatory role of different genomic sites is unraveled.

We also applied Phen-Gen to a study comprising 100 father-mother-child trio families with the child in each family suffering from intellectual disability symptoms[1]. Eleven families with variants implicated in recessive or X-mode inheritance were used in this evaluation. Of the reported genes, 81% (13 of 16) were ranked in the top ten in our prediction (**Supplementary Table 7**). In the original study, all mutations reported in the Single Nucleotide Polymorphism Database (dbSNP) or observed in the in-house data set were removed from further evaluation. Phen-Gen, on the other hand, allows rare (<1% minor allele frequency (MAF)) variants from dbSNP. When the original study criteria were adopted, the predictions improved further. Eight of eleven patients were assigned an implicated gene as the top gene, and all reported genes now ranked in the top five in the respective families (**Supplementary Table 7**).

We evaluated Phen-Gen against VAAST[8] and eXtasy[7], both of which rank genes or variants on the basis of only nonsynonymous mutations (**Fig. 1**). eXtasy under default settings ranks all common and rare variants. In ref. 7, it was also evaluated with rare variants (MAF <1%) separately. We show results under both scenarios. VAAST assigned top rank to an average of 14 genes per simulation, whereas Phen-Gen and eXtasy assigned a continuum of ranks with a lone gene assigned the top rank in each simulation. Phen-Gen assigned the causal gene top rank in 82% of cases for dominant disorders compared to 62% for VAAST and 24% for eXtasy. For recessive disorders, Phen-Gen assigned top rank in 97% cases compared to 78% for VAAST and 30% for eXtasy.

While Phen-Gen was in submission, PHEVOR[9] was published by the authors of VAAST. PHEVOR combines multiple disease and functional ontologies to improve the performance of genomic predictors such as VAAST. To evaluate its performance, 50 dominant and 50 recessive VAAST simulations were randomly chosen and the genes reprioritized using PHEVOR (**Supplementary Note**). Phen-Gen identified the causal gene in 90% of dominant and 88%

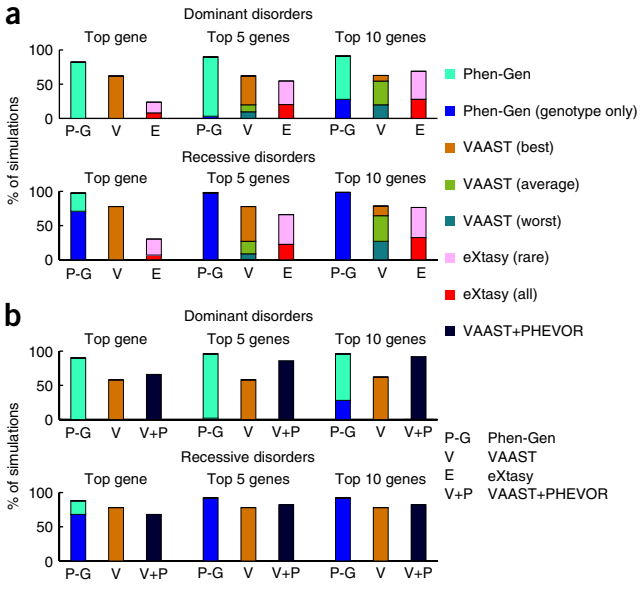

Figure 1 | Comparison with VAAST, eXtasy and VAAST+PHEVOR. The ability of each method to narrow down the true gene search within 1, 5 and 10 genes is depicted. (**a**) Split bars represent genotype prediction only or inclusion of disease symptoms for Phen-Gen and assignment of worst, average or best VAAST rank among multiple genes assigned to top rank by VAAST. For example, if VAAST assigns the true gene along with four other genes the same top rank, then the causal gene will be ranked as 1, 3 and 5 for best, average and worst, respectively. The three components of the VAAST bar reflect the performance across the three scenarios. The two components of eXtasy bars reflect its performance under the default settings and with the added advantage of discarding common variants (MAF >1%) from its input. (**b**) 50 dominant and 50 recessive simulations were randomly chosen for comparison with PHEVOR. For VAAST, only the best rank (among similarly ranked genes) is depicted. PHEVOR+VAAST bars highlight the added advantage of analyzing VAAST output in light of the phenotypic information by PHEVOR.

of recessive simulations, whereas VAAST+PHEVOR assigned the top rank in 66% and 68%, respectively (**Fig. 1**). In conclusion, Phen-Gen outperforms VAAST, eXtasy and VAAST+PHEVOR by 19–58%.

PHIVE[10] is another recently published method that integrates phenotypic information. It scores all exonic variants and matches human disease symptoms against a knockout mouse phenotype database using semantic similarity. In its publication, it was evaluated in a similar simulation framework, albeit with a different disease set of HGMD variants. The authors report its ability to assign the disease-causal gene first rank in 66% of cases for dominant and 83% of cases in recessive disorders. In comparison to PHIVE, Phen-Gen showed 16 and 13 percentage points' advantage in identifying the true causal gene for dominant and recessive disorders, respectively.

The impact of regulatory variants in congenital disorders is well established[13]. FunSeq[14] was recently published to predict the regulatory role of noncoding mutations. FunSeq's results using HGMD regulatory variants indicate a strong enrichment of damaging mutations, but only 18% of the damaging regulatory variants fall within its first filtration criteria. In contrast, Phen-Gen assigned damaging probabilities to 80% of these variants (**Supplementary Fig.** 7).

Phen-Gen highlights the advantage of integrating patient symptom information in understanding disease mechanism and works on both coding and noncoding variation.

METHODS

Methods and any associated references are available in the online version of the paper.

Note: Any Supplementary Information and Source Data files are available in the online version of the paper.

ACKNOWLEDGMENTS

This work was supported by the Agency for Science, Technology and Research (A*STAR), Singapore. We thank Radboud University Nijmegen Medical Centre for sharing the 100 intellectual disability patient data sets, particularly J. de Ligt for his help with this data. We also thank S. Köhler for his help with Phenomizer, N. Jinawath for her help interpreting patient symptoms, and S. Prabhakar and N. Clarke for their comments on the genomic predictor. We thank S. Prabhakar, S. Davila, A. Wilm and R. del Rosario for their comments on the manuscript.

AUTHOR CONTRIBUTIONS

A.J. conceived of and designed the project, designed and implemented the analysis framework, implemented methods, conducted experiments, interpreted results, wrote the initial manuscript and revised and proofread the paper. S.A. implemented methods, conducted experiments, set up the web server and revised and proofread the paper. P.C.N. conceived of and designed the project, revised and proofread the paper and supervised the project.

COMPETING FINANCIAL INTERESTS

The authors declare no competing financial interests.

1. de Ligt, J. *et al. N. Engl. J. Med.* **367**, 1921–1929 (2012).
2. Yang, Y. *et al. N. Engl. J. Med.* **369**, 1502–1511 (2013).
3. Cordero, J.F. *N. Engl. J. Med.* **352**, 2032 (2005).
4. Amberger, J., Bocchini, C.A., Scott, A.F. & Hamosh, A. *Nucleic Acids Res.* **37**, D793–D796 (2009).
5. Chakravarti, A. *Genome Res.* **21**, 643–644 (2011).
6. Köhler, S. *et al. Am. J. Hum. Genet.* **85**, 457–464 (2009).
7. Sifrim, A. *et al. Nat. Methods* **10**, 1083–1084 (2013).
8. Yandell, M. *et al. Genome Res.* **21**, 1529–1542 (2011).
9. Singleton, M.V. *et al. Am. J. Hum. Genet.* **94**, 599–610 (2014).
10. Robinson, P.N. *et al. Genome Res.* **24**, 340–348 (2014).
11. Stenson, P.D. *et al. Hum. Genet.* **133**, 1–9 (2014).
12. Fu, W. *et al. Nature* **493**, 216–220 (2013).
13. Visel, A. *et al. Nature* **464**, 409–412 (2010).
14. Khurana, E. *et al. Science* **342**, 1235587 (2013).

ONLINE METHODS

Gene list. We aimed to capture four popular gene lists (Consensus CDS, RefSeq, Ensembl and UCSC known). Incomplete transcripts were discarded in each database, and only protein-coding genes were considered. Alternatively spliced transcripts reported in the same data source were assigned to the same gene. The mapping from the first three databases to the UCSC known gene list was downloaded and used to merge gene names across data sources. Additionally, two genes were merged if any of their isoforms exhibited greater than 95% identity in the exon sequence in the same orientation[15]. Finally, an in-house mapping used for identifying alternate isoforms in the SIFT database was employed[16]. The final gene list comprised 26,803 protein-coding genes with 11.4 gene or transcript identifiers reported per gene on average. This gene set was employed in all the experiments in the manuscript, and any downloaded gene identifier was translated to this set.

Variant prediction. For the coding predictor, each called variant in the patient's genome (or exome) is evaluated if it lies within the coding regions in a reported transcript of the aforementioned gene list or if it falls within the splice-site definition of the intron-exon boundary. The coding variants are further subcategorized as start-loss, stop-gain, stop-loss, splice site, nonsynonymous, synonymous or indel. Each variant is assigned a probability of deleteriousness based on its highest estimated damaging impact. For the genomic predictor, all coding and noncoding variants are analyzed for their putative functional role.

Nonsynonymous variants. Nonsynonymous mutations are probably the best-studied class of damaging mutations, and a plethora of literature has been written and algorithms developed to evaluate their damaging impact. For our prediction we combined two commonly used algorithms: SIFT[16] and PolyPhen-2 (ref. 17). The aim here is to estimate the probability of a nonsynonymous mutation given its SIFT and PolyPhen-2 scores. We employed a positive and neutral data set to estimate the empirical distribution of these scores both individually and in conjunction. The positive set comprised disease-causal nonsynonymous mutations from the Human Gene Mutation Database (HGMD)[11]. The neutral set contained nonsynonymous substitutions in the human reference genome with respect to the ancestral sequence as inferred from the human-chimp-gorilla exome alignment. Only the loci where both chimp and gorilla sequence aligned and agreed on the allele were considered. The two distributions were combined using Bayes's rule with prior probability of a nonsynonymous variant being damaging 0.67 (ref. 18). The two algorithms exhibit general agreement (**Supplementary Fig. 2**). Hence the two ends of the spectrum where the predictions disagree are quite sparse. The posterior probability in these bins was interpolated using the geometric mean of their nearest neighbors. PolyPhen-2 predictions tend to average out within each bin; adding SIFT scores helps differentiate and improve the probability estimates within each bin. The continuum of predicted probabilities can be thresholded to achieve 91% accuracy with less than 2.1% false positives, which compares favorably with MutationTaster[19] at 87% accuracy and 4% false positive rate using the same data. It needs to be emphasized though that the downstream analysis uses the probability estimates and not the binary predictions.

Splice-site variants. Exon-intron boundary information was extracted for all the transcripts in the gene list from their respective databases. Mutations in the 8-bp locus surrounding the donor site or the 3-bp locus surrounding the acceptor site (**Supplementary Fig. 3**) were considered splice disrupting. In particular, the 2 bp at the start and end of an intron tend to be more conserved and hence were treated separately[20]. To estimate the probability of deleteriousness of a mutation affecting splicing boundaries, we employed splice-site disease-causal mutations from HGMD as a positive set. The neutral set contained common mutations in dbSNP with minor allele frequency (MAF) greater than 30% within the defined sites. The prior probability of a splice-site mutation being damaging was estimated by the reduction in the number of common mutations at these sites in comparison to the whole genome. The rationale was that the mutation rate is assumed to be constant in a random subset of the genome, and this reduction in common mutations is attributed to prior mutations being pruned out by negative selection. The splice-site definition fails to capture 8% of mutations reported in HGMD (with another 1% lying outside our gene list). A closer examination of these false negatives reveals that most of these sites are more than 10 bp away from our defined exon-intron boundaries. Some of these could reflect variability in transcript annotation; however, others could potentially be introducing alternate splice sites that would not be represented in the prediction.

Start-loss, stop-gain and stop-loss variants. Start- and stop-codon–altering mutations and nonsense mutations are highly deleterious and in most analysis are assumed to be damaging[21]. We confirmed this hypothesis by computing the relative decrease in common mutations at these sites with respect to the complete genome. Once again, common mutations (MAF >30%) in dbSNP were used, and these sites were defined using our gene set. Our analysis reveals that these mutations are highly likely to be damaging with probability 0.999.

Small insertions and deletions. To estimate the potential damaging impact of a genic indel, we first classify them as either frameshift or nonframeshift. A different predictor is used for each class. In both cases, the respective disease-causal indels from HGMD constitute the positive set. The neutral set comprises common mutations from dbSNP (MAF >30%). The prior probability of a coding indel being damaging is estimated using 54 unrelated whole-genome sequencing samples made publicly available by Complete Genomics Inc. The data set revealed a strong exonic bias in indel calls, with 20% of indels located within 4% of the genome annotated as coding genes. To correct for this bias, we compared the enrichment of rare indels (MAF <5%) and common indels (MAF >30%) within and outside the genes. The assumption being that both rare and common indels are affected equally by the coding bias. On the basis of this computation, the prior probability of a genic indel being damaging was estimated to be 0.0787. This is a weak prior, and the true value is likely to be higher. However, because of a higher false positive rate in calling indels (in comparison to SNPs), it would be prudent to err on the conservative side. Further, the weak prior is rescued by strong observation in both indel categories. All frameshift indels are assigned the probability of deleteriousness on the basis of the empirical distribution of its positive and neutral set combined using Bayes's rule. Nonframeshift indel predictions are further refined by incorporating the importance of the affected locus (based on its tolerance to single-nucleotide mutations).

doi:10.1038/nmeth.3046

Genomic variants. Next, we aimed to estimate the putative functional role of all genomic variants. To this end, conservation, putative regulatory interactions and proximity to genes were used to annotate the variants (**Supplementary Fig. 4**). Both GERP++[22] and PhyloP[23] (threshold 1.445) were used to define evolutionarily conserved sites. ENCODE computational predictions for transcription factor binding sites and experimental annotations for DNase-hypersensitive sites were included. Proximity to gene annotations (including coding sequence, UTRs and 70 bp at the start and end of each intron) was incorporated.

A key statistical challenge in estimating the functional role of noncoding mutations is the dearth of disease-causal regulatory mutations in public data sets. Further, most studies focus on coding variants, and hence dbSNP has accumulated a higher number of these variants over time. To correct for both these shortcomings, we employed two positive and two neutral data sets. Disease-causal regulatory mutations in HGMD and reported GWAS hits (downloaded from NCBI) constituted the positive sets. The neutral sets contained common SNPs in dbSNP and common SNPs in publicly available unrelated sample data from Complete Genomics Inc. (MAF >0.30), respectively. Ten thousand permutations were performed, and each positive and neutral data set was randomly selected with equal probability. Each selected data set was subsampled, in each permutation, to estimate confidence intervals (**Supplementary Fig. 5**). The positive and neutral empirical distributions thus estimated were combined within Bayes's rule. The prior probability of a random mutation in our annotated regions being damaging was estimated to be 0.0688. In addition to the aforementioned annotations, we also considered further annotations including GUMBY[24], noncoding RNA from GENCODE[25], microRNA[26] and G+C content[27]. The technical difficulty in embracing more annotations stems from the small size of the positive sets. Adding more annotations increases the number of bins exponentially. This dilutes the signal within each bin, making it more susceptible to stochastic noise. GUMBY is stringent in its conservation threshold and thus quite accurate but not all-encompassing to all functional regions. Furthermore, 99.65% of GUMBY conserved sites overlapped with GERP++. MicroRNA-predicted loci[28] and GENCODE annotations[29], despite their well-established epigenetic role, were not well represented in our positive sets. G+C content was suggestive of the regulatory role when only HGMD was used as the positive set; the predictive power disappeared when both positive sets were employed. This could potentially reflect the enrichment of *de novo* mutations in the HGMD data set, as mutation rate across the genome tends to correlate with G+C content[27]. These predictors can be further interrogated and perhaps rescued with increasing size of regulatory variant data sets.

Pooling. The estimated loss of function at the genic level is predicted by pooling damaging variants within each gene considering the most damaging predicted variants for maternally and paternally inherited chromosomes. If the haplotype phase information is not available, the first and second highest variants are considered under the assumption that they lie on opposite chromosomes. Noncoding mutations are assigned to the nearest gene within 50 kb. This criterion is similar to conservative settings in GREAT[30] and assumes potential *cis*-regulatory impact of these variants on the respective genes. The inheritance pattern of the variants is compared against the disease inheritance pattern. For small pedigrees (such as trios or quartets), only variants consistent with this pattern are evaluated. For larger pedigrees, the flexibility to allow for nominal inconsistencies is permissible. This leeway is to account for potentially undiagnosed patients, incomplete penetrance, low coverage and possible error in variant calls. Common variants are omitted from this pooling. For the prediction, any variant with reported MAF above 1% in the 1000 Genomes[31], National Heart, Lung, and Blood Institute Exome Sequencing Project (NHLBI ESP) or dbSNP[32] version 135 is deemed common and excluded from consideration as the etiological variant. The analysis allows for the user to discard or incorporate variants inconsistent with the pedigree. Unless *de novo* mutation is the likely cause of the condition, the former is recommended.

Healthy individuals have been reported to harbor up to 100 damaging mutations[33]. The distribution of these so-called deleterious variants is not uniform across all genes, and certain genes (such as olfactory genes) are more likely to carry these loss-of-function variants. To account and correct for these incidental red herrings, we compute a null distribution of our predictor for each gene using the samples from 1000 Genomes. These individuals have not been reported to suffer from any disorders and represent a generic snapshot of human genetic variability across the globe. The pooled probability distribution of each gene is estimated under both the dominant and recessive inheritance pattern (**Supplementary Fig. 6**). For a patient, only genes harboring variants that exceed the 99th percentile of the corresponding null distribution are considered for downstream analysis. For example, more than 1% of 1000 Genomes samples carry rare variants in *CYP2C19* on both chromosomes with estimated damaging probability 0.88 or higher. Hence, for a recessive-disorder patient, *CYP2C19* will be considered as a candidate gene only if there are two variants within the gene that both have a damaging probability higher than 0.88. A key advantage of our approach, in the context of the method, is that we establish a continuum of predicted loss of functionality of each gene within healthy individuals.

Phenotypic prediction. The patient's disease symptoms are mapped to the Human Phenotype Ontology database using an in-house replica of Phenomizer[6]. The aim here is to match the patient's symptomatology to the list of known disorders and estimate the significance of each disease match. The Benjamini-Hochberg multiple testing–corrected *P* values are translated to probabilities assuming the disease set has a uniform prior.

$$P_{\text{disease}}(i) = \frac{\frac{1}{\#\text{ of disorders}} \times P(\text{disease match} \mid \text{true match})}{\left(\begin{array}{l} \frac{1}{\#\text{ of disorders}} \times P(\text{disease match} \mid \text{true match}) \\ + \frac{(\#\text{ of disorders} - 1)}{\#\text{ of disorders}} \times P(\text{disease match} \mid \text{false match}) \end{array} \right)}$$

$$P_{\text{disease}}(i) \approx \frac{\frac{1}{\#\text{ of disorders}}}{\frac{1}{\#\text{ of disorders}} + P_{\text{value}}(i)}$$

Each disease probability is assigned to all genes implicated in the literature for that disorder. If no genes are currently known, the

probability is distributed uniformly across all genes. Certain genes are known to affect multiple disorders. Pleiotropy is accounted for by combining all the assigned probabilities for a gene across the spectrum of disorders it has been reportedly involved in.

$$P_{\text{gene}}(j) = 1 - \prod_i (1 - P_{\text{disease}}(i)) \times \delta(i,j)$$

where

$$\delta(i,j) = \begin{cases} 1 & \text{if gene } j \text{ has been implicated for disease } i \\ 0 & \text{otherwise} \end{cases}$$

Thus far we have estimated the role of each gene by leveraging direct knowledge of their involvement in diseases with similar symptoms. Next we incorporate 'guilt by association' using evidence of their interaction with a known perpetrator. To gather this circumstantial evidence, a random walk with restart is conducted on the gene-gene interaction network. Each gene is selected as a starting point of the walk with probability P_{gene}. A restart probability of 90% is used for the walk. This translates to 90% of the phenotypically matched probability, a.k.a. 'guilt', retained by the initial gene and 10% of it permeated across its known associates, with stronger evidence of interaction leading to a higher probabilities.

Gene-gene interaction network construction. In the context of the method, the gene-gene interactions are not limited to physical interaction of genes. Rather, they reflect the ability of two genes to affect the same underlying biology and thus lead to the same (or similar) disorders and symptoms. This information is agglomerated across different sources including known involvement in the same pathway or ontology domains, data-mined reports of co-occurrence across publications and/or correlated coexpression among tissue types. The gene-gene interaction network is constructed by combining these sources in a framework inspired by ref. 34. A key difference is that the original study made binary predictions, thus representing an unweighted graph, whereas we construct a randomized graph with edge weights proportional to confidence in interaction. The network construction is as follows. All pairs of genes reportedly involved in the same pathway (REACTOME[35], KEGG[36], NCI-Nature[37]) are considered true interactions. This confidence stems from the manual curation process of these sources by domain experts. To improve recall of the network, we supplement the pathway information with additional data sources. The pathway-based interactions are used to evaluate the predictive power of data-mining approaches (BioGRID[38], STRING[39]), Gene Ontology domain annotations[40] ("Cellular Component," "Molecular Function" and "Biological Process") and gene coexpression (COXPRESdb[41]). These predictions are combined within a unifying framework in a manner similar to that in ref. 34 with prior probability of two random genes interacting estimated from pathway databases. A high-confidence (co-involvement probability ≥0.1) gene-gene interaction network was thus defined. In total, the network comprised 920,898 interactions.

For testing the efficacy of this network in representing genetic heterogeneity, gene pairs implicated for the same disorder were extracted from HGMD and OMIM (10,852 and 5,083, respectively). 31% and 39% of these pairs are represented by a direct edge in the network ($P << 10^{-16}$ on the basis of the distribution of random gene pairs), indicating that the probability of their involvement in similar diseases is well represented in the network and that the network is significantly enriched in true interactions, which bodes well in its efficacy to elucidate novel gene involvements in known disorders.

Disease-causal genes tend to play a more central role in the interactome. This is reflected in the gene-gene interaction network, where HGMD- and OMIM-implicated genes tend to have a higher number of edges ($P \leq 10^{-166}$ and $P \leq 1.8 \times 10^{-192}$, respectively).

Combined predictions. Assuming phenotypic and genotypic probability estimates are independent observations of the same underlying probability of involvement of a gene, we combine the two predictions for each gene within a Bayesian framework.

The probability that gene j is disease causal is given by

$$\frac{P_G(j) \times P_P(j)}{P_G(j) \times P_P(j) + (1 - P_G(j)) \times (1 - P_P(j))}$$

where $P_G(j)$ and $P_P(j)$ are the probability that gene j is disease causal on the basis of genotype data and phenotype data, respectively.

Computational efficiency. Exome sequencing routinely yields 20,000 variants per sample; the number increases to 4 million for whole-genome sequencing. We employ a simultaneous linear scan of the variant and annotation files. To speed up the process, we defined regions of interest using interval forests, with one tree per chromosome. Overlapping intervals were merged to define a sieve that represents 19% of the genome. This allows the implementation to quickly sift out the variants of interest, discarding the rest. To expedite the actual run-time execution, whenever possible, we moved the burden of computation to preprocessing and stored information in a binary format for faster reading. For example, for noncoding variants the database overlap information is encoded in 1 byte per interval.

The source code, preprocessed databases and executables are provided as a single downloadable package. This includes an in-house implementation of Phenomizer with limited functionality necessary for Phen-Gen. The source code is released under the GNU General Public License, so a computationally savvy user can make changes to incorporate further metrics of deleteriousness and improve on the model. We plan to periodically update the online and downloadable versions of Phen-Gen (http://phen-gen.org/) with each major release of the source databases. The software is also available as an online server for ease of use.

Simulating *in silico* patients. To evaluate Phen-Gen we generated *in silico* patients. For a given disorder, a patient's genetic data were created by adding a known disease-causal mutation from HGMD into a healthy individual with zygosity consistent with the reported disease inheritance pattern. These genomes on average harbor 4 million genomic variants, of which 24,000 are coding[42]. The patient's phenotypic data were generated on the basis of reported disease symptoms. Phen-Gen allows pedigree data, which considerably narrows down the search pool, but in the simulations we aimed for the extreme case in which only the lone patient information is available. In the first set of simulations,

doi:10.1038/nmeth.3046

765 diseases for which at least one causal variant was reported in HGMD and the disease symptoms were defined in OMIM[4] were extracted. These symptoms were used to define the patient's condition. Each causal variant was systematically spiked in each of the 1,092 individuals from 1000 Genomes data set in turn, and the remaining individuals were used to define the null distribution (**Table 1** and **Supplementary Tables 1** and **6**).

To evaluate Phen-Gen's performance in identifying the disease-causal gene with a compound heterozygous disease-inheritance pattern, a second set of simulations was conducted. In these, the general framework remained the same as before. But this time, instead of a single variant, two variants were added to the patient genome in a heterozygous state on opposite chromosomes. For these simulations, only recessive inheritance pattern disorders with at least two variants reported in (or near) the same gene were used, with a simulated patient generated for every pair of reported variants (**Supplementary Table 4**). In the case where one or both of the members of a spiked variant pair was noncoding, the genomic variant predictor was used (**Supplementary Fig. 8**).

To evaluate Phen-Gen's robustness to phenotypic heterogeneity, 44 disorders for which the symptom list and their frequency of occurrence has been compiled[6] were used. For each disorder, five medical histories were constructed by randomly sampling each symptom based on its frequency. The simulations were conducted in a similar manner as before, with the added caveat that every individual patient genome was evaluated five times, once with each medical history (**Supplementary Table 5**).

15. Pruitt, K.D. *et al. Genome Res.* **19**, 1316–1323 (2009).
16. Sim, N.-L. *et al. Nucleic Acids Res.* **40**, W452–W457 (2012).
17. Adzhubei, I.A. *et al. Nat. Methods* **7**, 248–249 (2010).
18. Kryukov, G.V., Shpunt, A., Stamatoyannopoulos, J.A. & Sunyaev, S.R. *Proc. Natl. Acad. Sci. USA* **106**, 3871–3876 (2009).
19. Schwarz, J.M., Rödelsperger, C., Schuelke, M. & Seelow, D. *Nat. Methods* **7**, 575–576 (2010).
20. Lewin, B. *Genes VIII* (Benjamin Cummings, 2004).
21. Price, A.L. *et al. Am. J. Hum. Genet.* **86**, 832–838 (2010).
22. Davydov, E.V. *et al. PLoS Comput. Biol.* **6**, e1001025 (2010).
23. Cooper, G.M. *et al. Genome Res.* **15**, 901–913 (2005).
24. Prabhakar, S. *et al. Genome Res.* **16**, 855–863 (2006).
25. Derrien, T. *et al. Genome Res.* **22**, 1775–1789 (2012).
26. Kozomara, A. & Griffiths-Jones, S. *Nucleic Acids Res.* **39**, D152–D157 (2011).
27. Smith, N.G.C., Webster, M.T. & Ellegren, H. *Genome Res.* **12**, 1350–1356 (2002).
28. He, L. & Hannon, G.J. *Nat. Rev. Genet.* **5**, 522–531 (2004).
29. Esteller, M. *Nat. Rev. Genet.* **12**, 861–874 (2011).
30. McLean, C.Y. *et al. Nat. Biotechnol.* **28**, 495–501 (2010).
31. The 1000 Genomes Project Consortium. *Nature* **467**, 1061–1073 (2010).
32. Sherry, S.T. *et al. Nucleic Acids Res.* **29**, 308–311 (2001).
33. MacArthur, D.G. *et al. Science* **335**, 823–828 (2012).
34. Wu, G., Feng, X. & Stein, L. *Genome Biol.* **11**, R53 (2010).
35. Matthews, L. *et al. Nucleic Acids Res.* **37**, D619–D622 (2009).
36. Kanehisa, M., Goto, S., Sato, Y., Furumichi, M. & Tanabe, M. *Nucleic Acids Res.* **40**, D109–D114 (2012).
37. Schaefer, C.F. *et al. Nucleic Acids Res.* **37**, D674–D679 (2009).
38. Stark, C. *et al. Nucleic Acids Res.* **34**, D535–D539 (2006).
39. Franceschini, A. *et al. Nucleic Acids Res.* **41**, D808–D815 (2013).
40. Ashburner, M. *et al. Nat. Genet.* **25**, 25–29 (2000).
41. Obayashi, T. *et al. Nucleic Acids Res.* **41**, D1014–D1020 (2013).
42. The 1000 Genomes Project Consortium. *Nature* **491**, 56–65 (2012).